Alexandria Engineering Journal (2016) 55, 723–729

HOSTED BY

Alexandria University

Alexandria Engineering Journal

www.elsevier.com/locate/aej
www.sciencedirect.com

ORIGINAL ARTICLE

Nanoparticles Ni electroplating and black paint for solar collector applications

J. El Nady [a,*], A.B. Kashyout [a], Sh. Ebrahim [b], M.B. Soliman [b]

[a] City of Scientific Research & Technological Applications (SRTA-City), Advanced Technology & New Materials Research Institute, P.O. Box 21934, Alexandria, Egypt
[b] Institute of Graduate Studies and Research, Materials Science Department, University of Alexandria, P.O. Box 832, Alexandria, Egypt

Received 26 May 2015; revised 17 November 2015; accepted 20 December 2015
Available online 17 February 2016

KEYWORDS

Black paint;
Instantaneous efficiency;
Nanoparticles Ni electroplating;
Aging tests

Abstract A nanoparticles layer of bright nickel base was deposited on copper substrates using electrodeposition technique before spraying the paint. IR reflectance of the paint was found to be around 0.4 without bright nickel layer and the reflectance increased to 0.6 at a Ni layer thickness of 750 nm. The efficiency of the constructed solar collectors using black paint and black paint combined with bright nickel was found to be better than black paint individually. After aging tests under high temperature, Bright nickel improved the stability of the absorber paint. The collector optical gain $F_R(\tau\alpha)$ was lowered by 24.7% for the commercial paint and lowered by 19.3% for the commercial paint combined with bright nickel. The overall heat loss $F_R(U_L)$ was increased by 3.3% for the commercial paint and increased by 2.7% for the commercial paint combined with bright nickel after the temperature aging test.

1. Introduction

Due to increasing interest in the exploitation of renewable energy sources, absorbers for solar thermal applications are becoming increasingly important. The efficiency of the photothermal energy conversion is strongly dependent on the optical properties of the absorber [1]. The absorber consists of an absorber plate (the substrate) which is coated with the paint coating. The absorber substrate must be made of a material with good thermal conductivity to transfer the heat to fluid. Copper is the most metal used as substrate as it has high thermal conductivity. The absorber coating is responsible for the conversion of UV and VIS radiation to heat [2]. A selective paint that has a minimum reflection in the solar spectrum (high absorptance) and maximum reflection in the thermal spectrum (low emittance) can achieve this objective [3].

Because of the generally high emittance, the main selection criterion of non-selective paint coatings has high absorptance, good durability and low cost [4]. For solar thermal applications, the paint material and substrate should not greatly change their physical and chemical properties within operation. This may has adverse affect on the solar absorptance and thermal emittance. Thin metal base layer is deposited onto absorber metal substrates to avoid the diffusion into the composite film during accelerated aging tests, which decreases the optical performance of the coatings [5]. Coating material

* Corresponding author.
Peer review under responsibility of Faculty of Engineering, Alexandria University.

http://dx.doi.org/10.1016/j.aej.2015.12.029

selection is the key to find the acceptable solution to overcome the inter diffusion and higher emittance problems in solar selective coatings [6].

The performance of the flat-plate collector with an absorber for photothermal conversion can be described by the conversion efficiency (η) [7,8]

$$\eta = F_R\tau\alpha - F_R U_L\left(\frac{T_i - T_a}{I}\right) \quad (1)$$

where η is the instantaneous efficiency of solar collector, F_R is the collector heat removal factor, α is the solar absorptance, τ is the solar transmission, U_L is the heat transfer coefficient, T_i is the inlet temperature of the transfer medium flowing into the collector, T_a is the ambient temperature, and I is the total irradiance onto the collector plane.

Thickness insensitive spectrally selective (TISS) paint coatings were prepared according to Orel et al. [9]. Pigments were dispersed in silicone resin binder imparting the TISS paint coatings high-temperature tolerance, excellent adhesion, UV resistance, flexibility and weather-durability, which make them suitable coatings for glazed or unglazed solar absorbers. Spectrally selective surfaces can be prepared on three different substrates using siloxane and epoxy/silicone resins as binders according to Orel et al. [10]. The method of application of paint influenced the final spectral selectivity. Better results were obtained when the paint was applied by draw bar coater due to the more homogeneous distribution of the applied over the substrate. It was found that the thermal emittance decreased by the decreasing the thickness of the applied paint.

This paper deals with the following: first, the deposition and optical characterization of a commercial black paint delivered by the manufacture (Al Gammal Gp., Egypt) will be investigated; this paint is based on siloxane resin binder and is appropriate for high temperature applications above 200 °C. Then the impact of electrodeposited nanoparticles bright Ni base layer on the optical properties of the commercial paint also will be investigated. Solar collector instantaneous efficiency testing will be covered in detail. The efficiency tests are accomplished according to ASHRAE 93 standard (American Society of Heating, Refrigerating and Air conditioning Engineers, INC.) [11]. Finally, aging tests will be conducted on the whole collector. The impact of temperature aging test on the optical properties of the absorber coatings and its effect on the efficiency of the collector will be discussed.

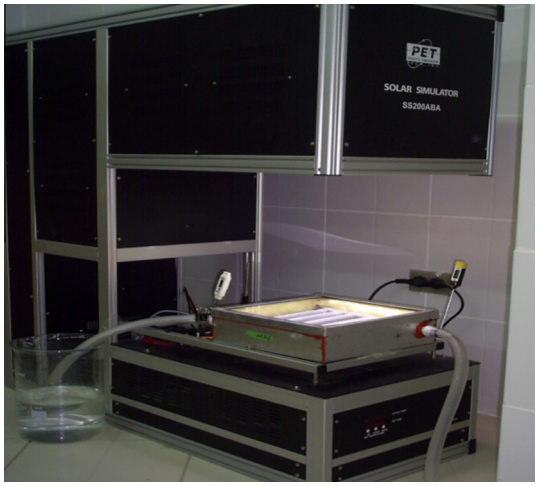

Figure 1 Setup for instantaneous efficiency measurement of the collector under illumination.

2. Materials and methods

Two prototypes of solar collectors: one with the black paint and the other with the black paint combined with the electroplated bright nickel base layer as absorbers are constructed. The gross area of the prototype is 27 × 27 cm^2, and the aperture area is 20 × 20 cm^2. The instantaneous efficiency measurements applied on the collector prototypes are performed using sun simulator (PET Photo Emission Tech., Inc. USA), with exposure area 20 × 20 cm^2 as shown in Fig. 1.

2.1. Sample preparation

Commercial black paint as received from Al Gammal Gp Company is applied on copper substrates and bright Ni base layer by spray deposition technique (Voylet H2000 spray gun, China). After spraying, the samples are cured at 180 °C for 45 min. to attain coating adequate thermal, weathering and mechanical resistance [10]. For Ni electroplating, DC regulated power supply as the power source and the copper substrate as cathode are used and a nickel sheet with a purity of 99.9% as anode is used. The composition of the electrolyte is shown in Table 1. Current density of 2 A/dm^2 and deposition time of 3 min are used. Nickel sulfate, low cost, commercially available material, is used as a source of nickel ions for deposition. For improving the brightness, cobalt sulfate is used. Boric acid serves as a weak buffer controlling PH of the solution. Ammonium chloride is used to improve both the cathode efficiency and the electrical conductivity of the solution [12].

2.2. Optical measurements of absorber material

The near-normal spectral reflectance of the samples was measured in the 0.2–0.9 μm wavelength range with (UV–visible evolution 600, Thermo). The specular reflectance is measured using varying angle specular reflectance accessory. Fourier Transform Infrared spectrophotometer (FTIR, Berkin Elmer) is used to measure near normal reflectance in the 2.5–29 μm wavelength range. From these measurements of specular reflectance, the solar absorptance (α) and thermal emittance (ε) behavior could be evaluated [13]. The main contents of the paint coating are investigated in the range from 400 to 4000 cm^{-1} using (Shimadzu FTIR-8400 S, Japan).

Table 1 Chemical composition for bright Ni deposition (at room temperature).

Material	Condition (g/l)
$NiSO_4{\cdot}7H_2O$	124
H_3BO_3	30
$CoSO_4{\cdot}7H_2O$	15
NH_4Cl	37

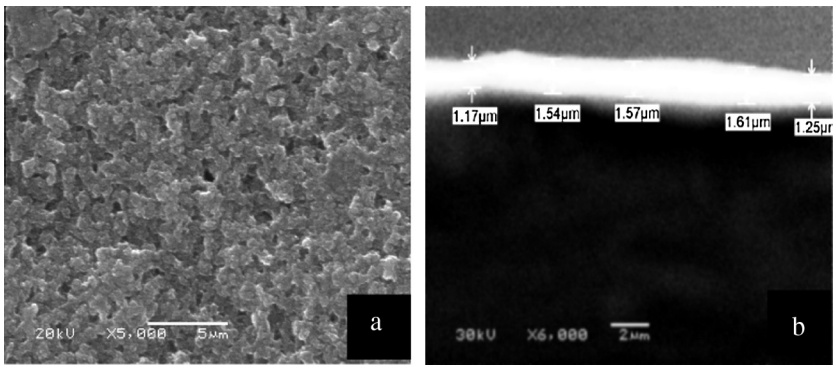

Figure 2 SEM of as-received black paint; (a) plain image, and (b) cross section of sprayed paint.

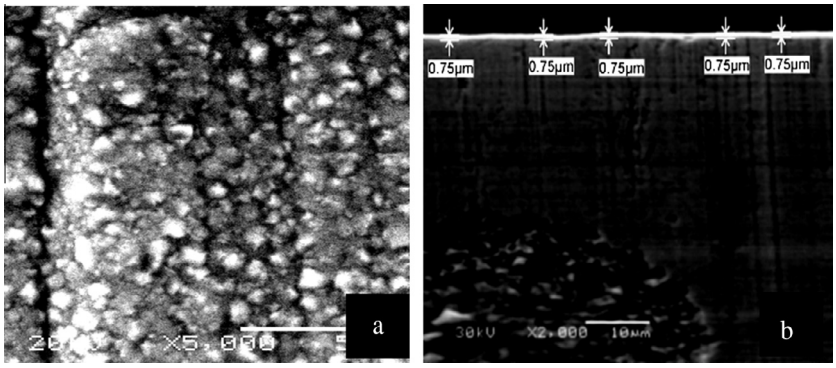

Figure 3 SEM of electroplated bright nickel; (a) plain image, and (b) cross section of sprayed paint.

2.3. Non-optical measurements of absorber material

The surface morphology and thickness of all absorber samples are studied with (JEOL, JSM-6360 LA) scanning electron microscope (SEM). Transmittance electron microscope (TEM) (JEOL TEM 1230, Japan) operating at 120 kV is used to compare the paint structure before and after the temperature aging test. Paint is stripped out from Cu substrate and suspended in ethanol and then spread on the Cu grid for the TEM measurement. The crystal structure of the paint coating and the bright Ni base layer samples are investigated with X-ray 7000 Schimadzu diffractometer using a Cu Kα target at 30 keV and 30 mA. Thermal stability of the paint is examined using (Shimadzu TGA – 50, Japan). The crystallite size can be determined from the broadening of corresponding X-ray spectral peaks by Scherrer formula [14].

$$L = K\lambda/(\beta\cos\theta) \quad (2)$$

where L is the crystallite size, λ is the wavelength of the X-ray radiation (Cu $K_a\alpha$ = 0.15418 nm), K is usually taken as 0.89, and β is the line width at half-maximum height.

The collector prototypes are subjected to an accelerated aging test for 200 h in an air oven (Carbolite S30, 2RR, England) at a temperature of 220 °C.

3. Results and discussion

3.1. Morphology of the black paint and bright Ni base layer

The morphology of the sprayed black paint on Cu substrate is investigated using SEM as shown in Fig. 2(a). Small voids are randomly distributed between the paint grains. These voids are possibly due the evaporation of the solvent during curing [15,16]. Fig. 2(b) shows a cross-sectional SEM photograph of the sprayed paint. The thickness ranged from 1.1 to 1.6 μm. The morphology of the electroplated bright Ni base layer with the electrolyte bath conditions (Table 1) is shown in Fig. 3(a). The crystals appear to be homogenous nanoparticles agglomerated with an average size of 500 nm are dispersed regularly. Fig. 3(b) shows cross-sectional SEM photograph for electroplated bright Ni base layer. A regular thin film is obtained and the thickness of the electroplated layer is about 750 nm.

3.2. Commercial black paint and bright Ni base layer structure

Fig. 4 illustrates the FTIR spectrum of the commercial paint as received. FTIR spectrum presents the OH absorbance band around 3440 cm^{-1}. The bands around 1099 and 800 cm^{-1} are associated with the antisymmetric stretch and symmetric stretch of the Si—O—Si (siloxane) linkages [10,15,17]. The band at 970 cm^{-1} is attributed to Si—OH bond [18]. The bands at 2856 cm^{-1} of CH_2 stretching [19] and at 2918 cm^{-1} of —CH_3 gp are observed [20]. The band at 1382 cm^{-1} is attributed to (C—H) bond [21]. The bands at 1687 cm^{-1} and 1620 cm^{-1} are attributed to C=C (aliphatic) [22]. The band at 1229 cm^{-1} belonged to the C—O—C bonds [23,24]. From the FTIR, we conclude that the commercial paint may be formulated from a polymer which consists of a hydrocarbon chain linked with silicone resin or silica.

The XRD of the black paint is shown in Fig. 5. It appears that the black paint has a high degree of crystallinity. Peaks at 25.3°, 29.2°, 31.9° and 33.2° are corresponding to

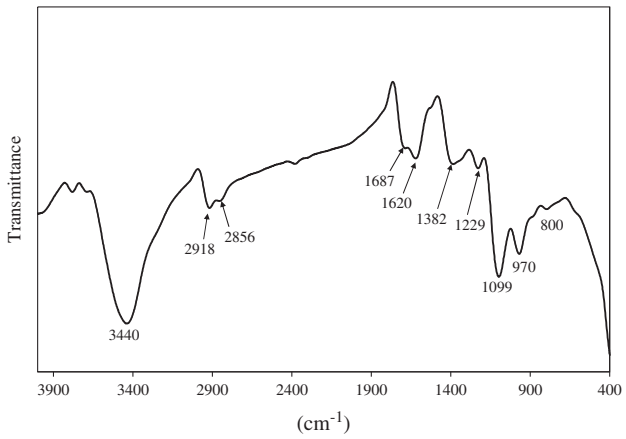

Figure 4 FTIR spectrum of the as-received black paint.

SiO_2-monoclinic (JCPDS, card No. 00-014-0654). Peaks at 20.4°, 26.3°, 49.5°, 55.1° and 65.8° are corresponding to SiO_2-hexagonal (JCPDS, card No. 00-011-0252). Also peaks at 43.2°, 63.4° and 97.7° are corresponding to SiC-cubic (JCPDS, card No. 00-049-1623). Peaks at around 27.4°, 36.5°, 41.2°, 60.9°, 75.7°, 80.4° and 89.3° are corresponding to SiC-rhombohedral (JCPDS, card No. 01-089-1977) and finally peaks at 26.3° and 53.5° are corresponding to carbon (JCPDS, card No. 41-1487) [25]. These results confirm the presence of silicone resin or silica in the black paint as indicated from FTIR in Fig. 4. XRD analysis of the Ni phases obtained by electroplating technique is shown in Fig. 6 [26]. The electroplated Ni is fcc nickel (JCPDS, card No. 03-1051). It appears that the preferred orientation for electroplated Ni is (1 1 1).

3.3. Thermal Gravimetric Analysis (TGA) of the commercial black paint

The black paint does not contain any water since no mass loss occurs up to 223 °C as indicated by TGA curve (Fig. 7) [18]. The degradation process of the black paint occurs at two steps (around 223 °C and 391.5 °C). The first weight loss step at 223 °C may be due to the decomposition of the polymer and solvent used in the paint. The second weight loss step at 391.5 °C may be due to the decomposition of the Si—O bond. The high thermal stability of this paint could be attributed to the higher bond dissociation energy of Si—O bond [27]. Also the residue at the temperature 600 °C is low (~20%) which may be due to that the silicone or silica content present in the paint is relatively small [28].

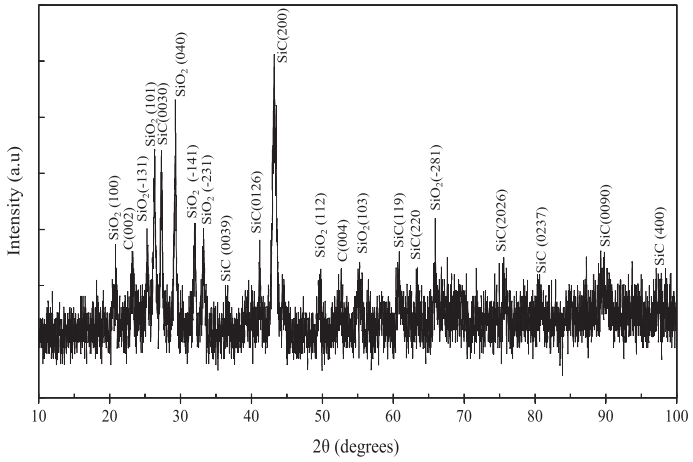

Figure 5 XRD pattern of the as-received black paint.

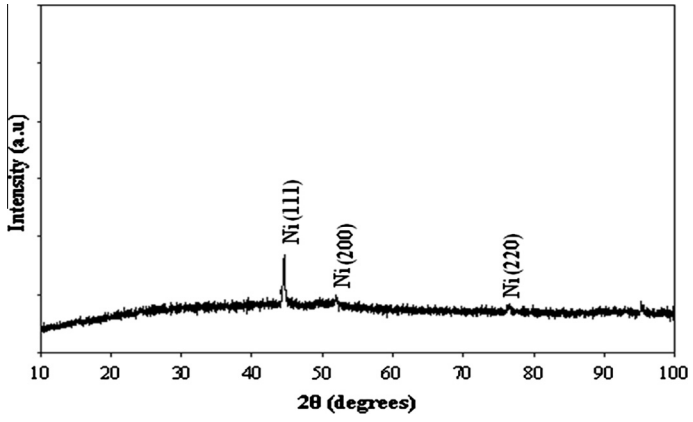

Figure 6 XRD of the electroplated bright nickel as indicated in Table 1.

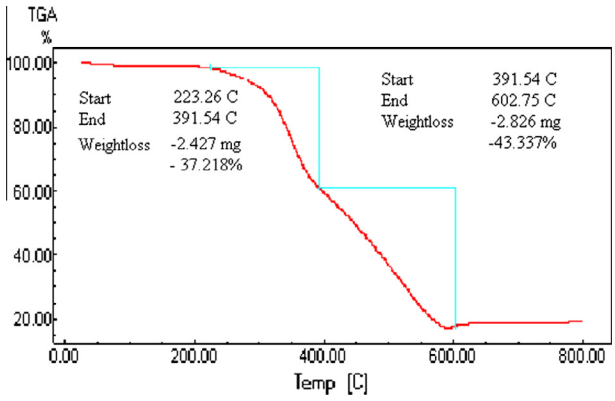

Figure 7 TGA thermograms of the as-received black paint.

3.4. Optical properties of the absorber coatings

The black paint shows low reflectance in the UV–visible region, indicating a high solar absorptivity. In contrast, it shows comparable high reflectance in the IR region and it has low emittance in the thermal range as shown in Fig. 8. From these results, it can be concluded that this paint has a moderate selectivity as its optical behavior changes between the two spectral ranges (UV–visible and IR). The maximum possible difference between the absorption of the solar radiation and transmittance of the thermal (i.e. infrared) radiation is achieved by optimizing the absorber coating's thickness (1–2 μm) [29,30]. The reflectance in IR range of the paint with the presence of bright Ni base layer is higher compared to the paint without the presence of bright Ni as shown in Fig. 8. It can be seen that the reflectance of the paint is around 0.4 without the deposited bright Ni layer and the reflectance becomes around 0.6 at 7.8 μm when the bright Ni has been deposited on the substrate. This confirms that the bright Ni layer decreases the thermal emittance of the black paint [6]. The absorbers samples are aged in the oven at 220 °C for 200 h. The optical properties of the paint are changed slightly due to its good stability and a decrease of about 0.1% of IR reflection is detected as shown in Fig. 8 [31]. The reflection of the paint with bright Ni base layer after the temperature aging test is also presented in Fig. 8. It appears that the paint is not affected by the temperature aging test. The bright Ni layer prevents the diffusion of Cu particles into the paint layer [6].

Fig. 9 shows TEM photograph for the black paint before and after temperature aging test. It appears that the pigment particles are dispersed in the binder matrix before temperature aging test. After temperature aging test, it appears the evaporation of the resin binder and agglomeration of the pigment particles.

3.5. Instantaneous efficiency measurements

The instantaneous efficiency test of the collectors is performed using a standard solar simulator. Four inlet temperatures are used: the ambient temperature, outlet temperature, mass flow rate and illumination intensity are recorded to obtain the efficiency curve using Eq. (1). The collector parameters namely $F_R(\tau\alpha)$ (the intercept) and $F_R(U_L)$ (the slope) are estimated using the efficiency curve. It is clear that $F_R(\tau\alpha)$ that describes the collector optical gain which depends on the optical properties of the absorber coating is almost the same for the two collectors, as shown in Fig. 10. $F_R U_L$ for the collector with black paint combined with bright Ni base layer (8.561 W/m^2 K) is lower than that for the collector with black paint only (9.740 W/m^2 K). This may be due to the presence of bright Ni base layer reduces the emittance of the black paint as shown in Fig. 8. As the absorber coating emittance decreased, $F_R U_L$ is decreased due to the lowering radiation losses from the absorber, and the efficiency of the collector is improved consequently [32].

The two collectors are aged in the oven at 220 °C for 200 h [33]. For the commercial paint, the efficiency of the collector is decreased as shown in Fig. 10. $F_R(\tau\alpha)$ is decreased from 0.677 to be 0.5015 and $F_R U_L$ is increased from 9.740 to 10.05 W/m^2 K. For the black paint with Ni base layer, as shown in Fig. 10, the efficiency after temperature aging test is decreased. $F_R(\tau\alpha)$ is decreased from 0.677 to 0.546, and $F_R U_L$ is increased from 8.561 to 8.788 W/m^2 K. It appears that

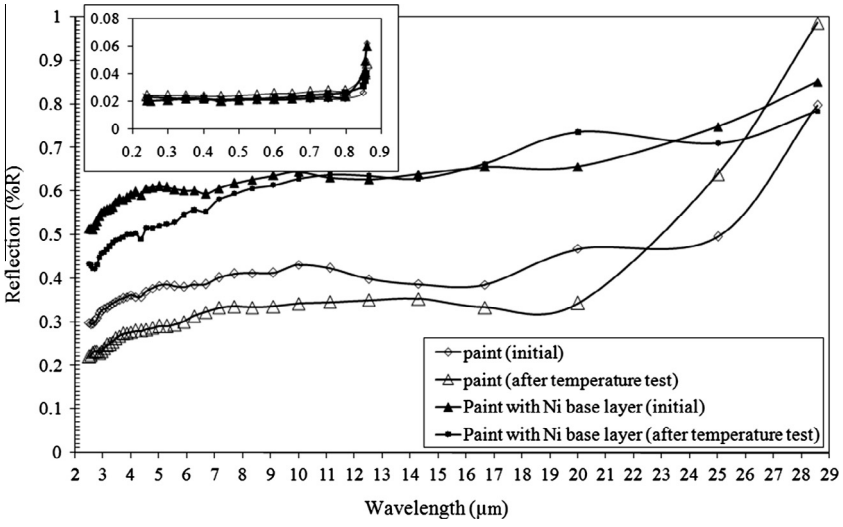

Figure 8 Specular reflectance of the black paint with and without a base layer of bright nickel in the UV–visible region and IR.

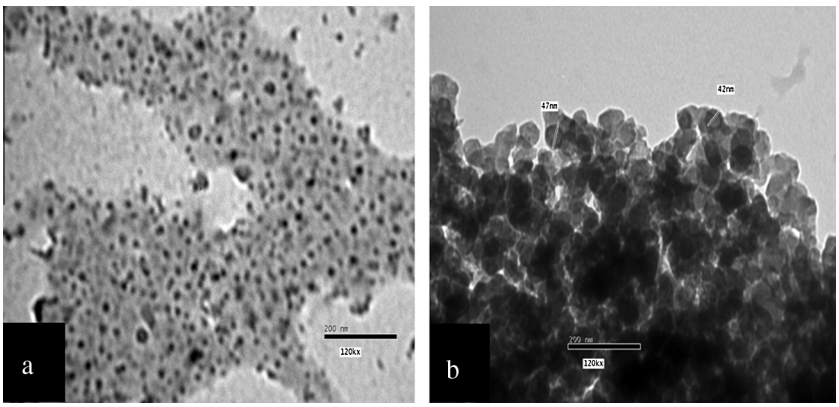

Figure 9 TEM photograph of black commercial paint as received: (a) before temperature aging test and (b) after temperature aging test.

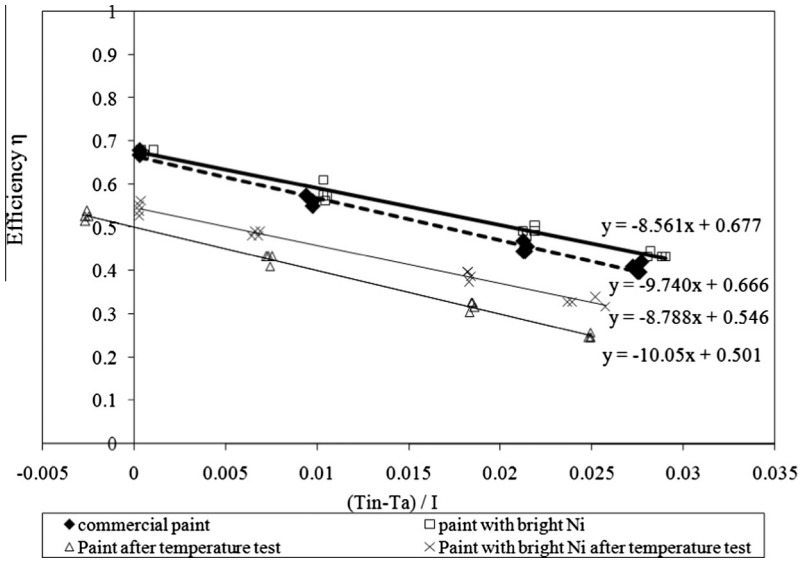

Figure 10 Instantaneous efficiency curves for the two collectors without and with bright Ni.

the collector with commercial paint combined with bright nickel base layer has a lower degradation effect in its parameters than the collector with commercial black paint which confirms the prevention role of the nickel layer. The optical gain $F_R(\tau\alpha)$ is lowered by 24.7% and 19.3% for the commercial paint and the commercial paint combined with bright Ni base layer, respectively. The overall heat loss $F_R U_L$ is increased by 3.3% and 2.7% for the commercial paint and commercial paint combined with bright Ni base layer, respectively.

4. Conclusions

Although commercial paint has good thermal stability, a layer of electrodeposited bright Ni decreased the thermal emittance and improved the thermal stability of the commercial paint. IR reflectance of the paint was around 0.4 without the deposited bright Ni layer and the reflectance became around 0.6 at 7.8 μm when the bright Ni had been deposited on the substrate. After temperature aging test, the collector optical gain $F_R(\tau\alpha)$ was lowered by 24.7% and 19.3% for the paint and the paint combined with bright Ni base layer, respectively. Also, the overall heat loss $F_R(U_L)$ was increased by 3.3% and 2.7% for the paint and the paint combined with bright Ni base layer, respectively.

References

[1] D.E. Roberts, A figure of merit for selective absorbers in flat plate solar water heaters, Sol. Energy 98 (2013) 503–510.
[2] A. Duta, L. Isac, A. Milea, E. Ienei, D. Perniu, Coloured solar-thermal absorbers – a comparative analysis of cermet structures, Energy Proc. 48 (2014) 543–553.
[3] L.S. Perse, M. Mihelcic, B. Orel, Rheological and optical properties of solar absorbing paints with POSS-treated pigments, Mater. Chem. Phys. 149–150 (2015) 368–377.
[4] T. Matuska, V. Zmrhal, J. Metzger, Detailed modeling of solar flat-plate collectors 1 with design Tool Kolektor 2.2, in: Eleventh International IBPSA Conference, Glasgow, Scotland, 2009.
[5] I. Jerman, M. Kozelj, B. Orel, The effect of polyhedral oligomeric silsesquioxane dispersant and low surface energy additives on spectrally selective paint coatings with self-cleaning properties, Sol. Energy Mater. Sol. Cells 94 (2010) 232–245.
[6] M. Farooq, I.A. Rajab, Optimization of metal sputtered and electroplated substrates for solar selective coatings, Renew. Energy 33 (2008) 1275–1285.

[7] T.N. Anderson, M. Duke, J.K. Carson, The effect of color on the thermal performance of building integrated solar collectors, Sol. Energy Mater. Sol. Cells 94 (2010) 350–354.
[8] C.N. Tharamani, S.M. Mayanna, Low-cost black Cu–Ni alloy coatings for solar selective applications, Sol. Energy Mater. Sol. Cells 91 (2007) 664–669.
[9] B. Orel, H. Spreizer, L. SlemenikPerse, M. Fir, A. SurcaVuk, D. Merlini, M. Vodlan, M. Kohl, Silicone-based thickness insensitive spectrally selective (TISS) paints as selective paint coatings for coloured solar absorbers (Part I), Sol. Energy Mater. Sol. Cells 91 (2007) 93–107.
[10] Z.C. Orel, M.K. Gunde, A. Lencek, N. Benz, The preparation and testing of spectrally selective paints on different substrates for solar absorbers, Sol. Energy 69 (2000) 131–135.
[11] ANSI/ASHRAE Standard 93-2003, Methods of Testing to Determine Thermal Performance of Solar Collectors, ASHRAE Inc., 1791 Tullie Circle, Ne, Atlanta, GA30329, 2003, ISSN: 1041-2336.
[12] O. Sadiku-Agboola, E.R. Sadiku, O.I. Ojo, O.L. Akanji, O.F. Biotidara, Influence of operation parameters on metal deposition in bright nickel-plating process, Portugaliae Electrochim. Acta 29 (2) (2011) 91–100.
[13] C.G. Granqvist, Solar energy materials, Adv. Mater. 15 (21) (2003) 1789–1803, Wiley-VCH VerlagGMbH&Co.KGaA, Weinheim.
[14] D.D. Dunuwila, Ch.D. Gagliardi, K.A. Berglund, Application of controlled hydrolysis of titanium (IV) isopropoxide to produce sol–gel derived thin film, Chem. Mater. 6 (1994) 1556–1562.
[15] Y.-Y. Yu, C.-Y. Chen, W.-C. Chen, Synthesis and characterization of organic–inorganic hybrid thin films from poly(acrylic) and mono dispersed colloidal silica, Polymer 44 (2003) 593–601.
[16] Z.C. Orel, B. Orel, Thermal stability and cross-linking studies of diisocyanate cured solar absorptance low-emittance paint coatings prepared via coil-coating process, Sol. Energy Mater. Sol. Cells 36 (1994) 11–27.
[17] P. Richharia, Microstructural investigations of a textured black brass selective surface, Thin Solid Films 272 (1996) 7–9.
[18] O. Topcuoglu, S.A. Altinkaya, D. Balkose, Characterization of waterborne acrylic based paint films and measurement of their water vapor permeabilities, Prog. Org. Coat. 56 (2006) 269–278.
[19] G. Chen, S. Zhou, G. Gu, L. Wu, Modification of colloidal silica on the mechanical properties of acrylic based polyurethane/silica composites, Colloids Surfaces A: Physicochem. Eng. Aspects 296 (2007) 29–36.
[20] M. Kozelj, A.S. Vuk, I. Jerman, B. Orel, Corrosion protection of sunselect, a spectrally selective solar absorber Coating, by (3-mercaptopropyl) trimethoxysilane, Sol. Energy Mater. Sol. Cells 93 (2009) 1733–1742.
[21] N. Heiskanen, S. Jamsa, L. Paajanen, S. Koskimies, Synthesis and performance of alkyd–acrylic hybrid binders, Prog. Org. Coat. 67 (2009) 329–338.
[22] M.J. Danilich, D.J. Burton, R.E. Marchant, Infrared study of perfluorovinylphosphonic acid, per fluoroallylphosphonic acid, and pentafluoroallyldiethylphosphonate, Vib. Spectrosc. 9 (1995) 229–234.
[23] J.P. Matinlinna, L.V.J. Lassila, P.K. Vallittu, The effect of a novel silane blend system on resin bond strength to silica-coated Ti substrate, J. Dent. 34 (2006) 436–443.
[24] F.A. Settle, Handbook of Instrumental Techniques for Analytical Chemistry, Prentice Hall PTR, USA, 1997 (Chapter 15).
[25] P. Wang, Y. NuLi, J. Yang, Y. Zheng, Carbon-coated Si–Cu/graphite composite as anode material for lithium-ion batteries, Int. J. Electrochem. Sci. 1 (2006) 122–129.
[26] S.P. de Lima, V. Vicentini, J.L.G. Fierro, M.C. Rangel, Effect of aluminum on the properties of lanthana-supported nickel catalysts, Catal. Today 133–135 (2008) 925–930.
[27] S.-J. Park, F.-L. Jin, J.-R. Lee, Synthesis and characterization of a novel silicon-containing epoxy resin, Macromol. Res. 13 (1) (2005) 8–13.
[28] H.-S. Park, I.-M. Yang, J.-P. Wu, M.-S. Kim, H.-S. Hahm, S.-K. Kim, H.-W. Rhee, Synthesis of silicone-acrylic resins and their applications to super weather able coatings, J. Appl. Polym. Sci. 81 (2001) 1614–1623.
[29] Maki et al., Coating Compositions for Solar Selective Absorption Comprising a Thermosetting Acrylic Resin and Particles of a Low Molecular Weight Fluorocarbon Polymer, United States Patent, 4,426,465, 1984.
[30] J. Vince, A.S. Vuk, U.O. Krasovec, B. Orela, M.K. Ohl, M. Heck, Solar absorber coatings based on CoCuMnOx spinels prepared via the sol–gel process: structural and optical properties, Sol. Energy Mater. Sol. Cells 79 (2003) 313–330.
[31] E. Streicher, S. Fischer, W. Heidemann, H.-M. Steinhagen, Performance Model for Solar Thermal Collectors Taking into Account Degradation Effects, Universität Stuttgart, InstitutfürThermodynamik und Wärmetechnik (ITW), Germany, 2007.
[32] B. Hellstrom, M. Adsten, P. Nostell, B. Karlsson, E. Wackelgard, The impact of optical and thermal properties on the performance of flat plate solar collectors, Renew. Energy 28 (2003) 331–344.
[33] J.A. Duffie, W.A. Beckman, Solar Engineering of Thermal Processes, second ed., John Wiley & Sons, Inc., 1991.